Indian Journal of Pure & Applied Physics
Vol. 60, February 2022, pp. 163-170

Dielectric Barrier Discharge Effect on Capacitively Coupled RF Argon Glow Discharge

A Bouchikhi

University of Saida, Faculty of Technology, Department of Electrical Engineering, Saida 20000, Algeria

Received 25 November 2019; accepted 19 January 2022

In this work we study the effect of the dielectric barrier discharge (DBDs) on capacitively coupled radio frequency argon glow discharge at low pressure. Firstly, the property discharges are given without DBDs, commenced by means of which exists in the literature in order to validate our code numeric. The model is based on the drift-diffusion approximation. The results with DBDs are mostly affected by means of the surface charge concentrations and the gap voltage. Consequentially, the particle densities, electric potential and electric field, mean electron energy as well as the current densities are totally different compared to those obtained without dielectrics.

Keywords: RF glow discharge, Gauss's law, Dielectric barrier discharges, Capacitively coupled.

1 Introduction

The development technologies in DC and RF glow discharge[1-12] time after time opens on the new technique. Among which, we find the dielectric barrier discharge[13-16]. In starting application has a role to avoid the arc discharge in the reactor plasma, then to protect the material. After that, they utilized in vast domain; microelectronic, renewable energy and medicine. In particular, thin layer deposits, decomposition of CO_2 by catalyst system and treatment of the skin diseases.

So, the mathematical analyses of the physical and chemical mechanisms in the reactor discharge rest a still indispensable. The difference between the reactor with and without dielectric is about the gap voltage and the accumulation charged on the dielectrics. To well understand the physical phenomena in the presence of the dielectrics, we have been investigating the RF argon plasma by means a simple model that described by Lin & Adomaitis[17]. Subsequently, we have added to the system a dielectric for well illustrate the comparison, and give the morphology of the surface charge concentration and the gap voltage.

The outline of this paper is to well describe the mathematical model mostly in the accumulation of the charged on the dielectrics and the boundary conditions affect that is given in the section 2. The discussion results with and without dielectric are given in section 3. Terminate works report in conclusion in section 4.

2 Model description

The plasma processing reactors at low pressure by means complete model can be theoretically decayed to three submodels describing: (1) the surface reactions; (2) plasma physics; and (3) reactor model also named the plasma chemistry. The surface reaction model depends on illustrations of the solid state physics of the material under treatments, and plasma physics focusing on discharge structure, and reactor model is a natural addition of computational fluid dynamics simulation and is comparatively more advanced than the plasma physic model; consequently, the plasma physics submodel can be considered the link relating the three submodels.

The Boltzmann equation combined with Maxwell's equations as named as complete model, it will well describe the discharge physics. Nevertheless, all the parameter transports and rate coefficients hold in the Boltzmann distribution function may not be required for a particular modeling purpose.

A substitute fluid-kind formulation based on the moments of the Boltzmann equation may be employed to get information on the macroscopic characteristics of the discharge. These fluid kind approaches have had immense achievement in clearing the physics of the glow discharge, and the results can be similar to those created by techniques

*Corresponding author: (E-mail: bouchikhiabdelaziz1@yahoo.fr)

of the Monte Carlo particle code. In this paper, the model without dielectrics is similar to the modeling equations illustrated in[7] and the alterations according to[17] are approved for this RF discharge.

The corresponding discharge configurations taking into account the axial component x of the plasma between the plane-parallel electrodes without and with dielectric are displayed in Fig. 1 and 2, respectively.

Then, the fluid description is given by relations

$$\frac{\partial n_e}{\partial t}+\frac{\partial \Gamma_e}{\partial x}=S_e \ , \qquad \ldots (1)$$

$$\frac{\partial n_+}{\partial t}+\frac{\partial \Gamma_+}{\partial x}=S_+ , \qquad \ldots(2)$$

$$\frac{\partial \varepsilon_e n_e}{\partial t}+\frac{5}{3}\frac{\partial \Gamma_{e\varepsilon}}{\partial x}=S_{e\varepsilon} \qquad \ldots(3)$$

$$S_e=S_+=n_e N k_i \qquad \ldots(4)$$

$$\Gamma_e=-n_e\mu_e E-\frac{\partial D_e n_e}{\partial x} \ , \qquad \ldots(5)$$

$$\Gamma_+=n_+\mu_+ E-\frac{\partial D_+ n_+}{\partial x} , \qquad \ldots(6)$$

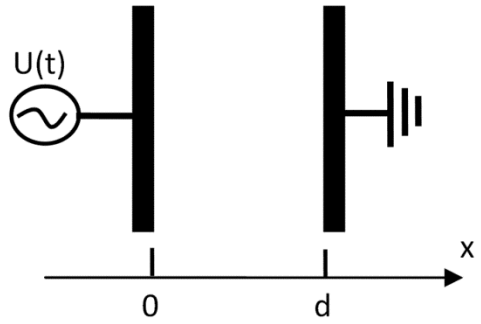

Fig. 1 — Discharge configuration without dielectrics.

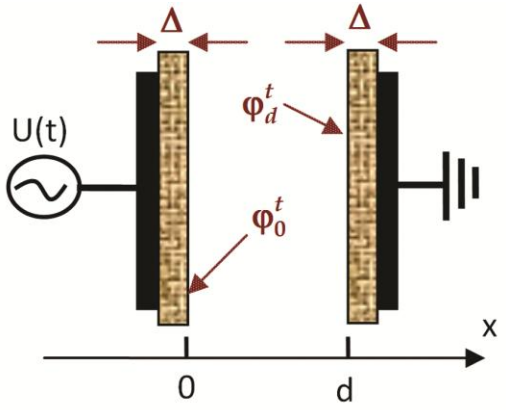

Fig. 2 — Discharge configuration with dielectrics, and φ_x^t is the electric potential at the dielectric side.

$$\Gamma_{e\varepsilon}=-n_e\varepsilon_e\mu_e E-\frac{\partial D_e n_e \varepsilon_e}{\partial x} \ , \qquad \ldots(7)$$

$$S_{e\varepsilon}=-e_o\Gamma_e E-S_{e\varepsilon}H_i \ , \qquad \ldots(8)$$

$$\frac{\partial^2\varphi}{\partial x^2}=-\frac{e_o}{\varepsilon_o}(n_+-n_e) \ , \qquad \ldots(9)$$

where n_e, n_+, and Γ_e, Γ_+ are the particle densities, and particle flux of electrons, ions, respectively, and their source term are S_e, S_+ . N denotes the neutral gas density. ε_e is the mean electron energy, $\Gamma_{e\varepsilon}$ is the electron energy flux, and the corresponding source term is $S_{e\varepsilon}$. φ is the electrostatic potential, and E is the electric field strength. μ_e, μ_+, and D_e, D_+, denote the mobilities and diffusion coefficients of electron and ions. ε_o and e_o are the permittivity of free space and elementary charge, respectively.

k_i is the ionization coefficient, and it is experimentally determined by Richards *et al.*[18]. The corresponding empirical expression is written in Equation 10.

$$k_i=\begin{cases} 8.7\times10^{-9}(T_e-5.3)\exp\left(-\dfrac{4.9}{\sqrt{T_e-5.3}}\right) \\ \\ 0 \end{cases}$$

if $T_e \succ 5.3$

if $T_e \le 5.3$ $\qquad \ldots(10)$

The boundary conditions at x=0 and x=d are: $\nabla_x n_{+,e}=0$ and $T_e=0.2$ eV. The discharge reactor is powered at x=0 by sinusoidal voltage $U(t)=U_a sin(2\pi ft)$. The initial densities are chosen as Gaussian form; $n_e=n_+=10^7+10^9(1-x/d)^2(x/d)^2$ cm^{-3}[19-20].

2. 1. Boundary conditions in the presence of the dielectrics

In the presence of the dielectrics, the particle flux of electron and ion[13] are written:

$$\Gamma_+.\nu=\frac{1-r_+}{1+r_+}\left(\left|n_+\mu_+E\right|+\frac{\upsilon_+^{th}n_+}{2}\right), \qquad \ldots(11)$$

$$\Gamma_e.\nu=\frac{1-r_e}{1+r_e}\left(\left|n_e\mu_e E\right|+\frac{\upsilon_e^{th}n_e}{2}\right), \qquad \ldots(12)$$

with ν is equal to -1 at x=0, and $\nu = 1$ at x=d, and $r_{e,+}$ is the reflection coefficient of electrons or ions . the thermal velocity of electrons or ions is given by:

$$\upsilon_{e,+}^{th} = \sqrt{\frac{8k_b T_{e,+}}{\pi m_{e,+}}} \quad . \qquad \ldots(13)$$

To discover the accumulation of surface charges on the dielectrics, the Gauss law[13-16] is applied:

$$\varepsilon_r \varepsilon_o E_{diel}(x,t).\nu - \varepsilon_o E(x,t).\nu = \sigma_s(x,t) \ , \qquad \ldots(14)$$

where $E_{diel}(x,t)$ is the electric field inside the dielectric and ε_r is their relative permittivity, and $E(x,t)$ is the electric field related to the gas discharge. To compute the electric potential at the dielectrics (φ_0^t and φ_d^t), we have employed Equation 14. The temporal evolution of the surface charge density $\sigma_s(x,t)$ begins from particle currents breakthrough the dielectrics and is expressed by Becker *et al.*[13]

$$\frac{\partial \sigma_s(x,t)}{\partial t} = e_o \sum_j \Gamma_j(x,t).\nu \ . \qquad \ldots(15)$$

The set of partial differential equations is discretized using the finite difference method. More clearly, the transport particle and energy equations have been discretized according to an exponential scheme[21-22]. The Poisson's equation has been spatial discretized by means of central difference technique. The both steps in time and space grids are taken uniform and constants.

3 Results and discussion

(a) Without dielectrics

In order to examine our code numeric developed in the framework, we have been investigating capacitive coupled radio frequency argon glow discharge in the same conditions as indicated by Lin & Adomaitis[17]. So, we have used the same geometry and transport parameters as well as the rate coefficients as proposed in[17], and they are mentioned in Table 1.

Comprehensive model and their results were given of capacitively coupled radio frequency gas glow discharges have been told in the literature[23,24].

The operating discharge is set to 1 torr gas pressure, 40 V forces amplitude and 2 cm inter-electrodes spacing. Three phases (0, $\pi/2$ and π) are chosen to illustrate the spatial distributions of the electric potential, electron density and electric field as well as electron temperature in the 2000[th] discharge cycle, which represent the limit cycle, *i.e.*, the steady-state of the discharge, and are given in Fig. 3. The obtained results are qualitatively agreed with numerous of the tale physical phenomena property of argon RF discharges [25,26] and are mostly well adapted to the results given by Lin & Adomaitis[17]. The main procedures utilised in our model and that given by Lin & Adomaitis are mentioned in the Table 2, which focus on the spatially step and the method employed.

Table 1 — Discharge configuration and argon physical characteristics applied in ccrf discharge

Symbol	Definition	Value
D	Electrode distance	2 (cm)
T_{gas}	Gas temperature	293 (K)
P	Pressure	1 (Torr)
U_a	Voltage amplitude	40 (Volt)
f	Frequency	13.56 (MHz)
μ_e	Electron mobility	3×10^5 ($cm^2\ v^{-1}\ s^{-1}$)
D_e	Electron diffusivity	12×10^5 ($cm^2\ s^{-1}$)
μ_+	Ion mobility	1.4×10^3 ($cm^2\ v^{-1}\ s^{-1}$)
D_+	Ion diffusivity	40 ($cm^2\ s^{-1}$)
H_i	Energy loss by ionisation	15.578 (eV)

The ion density is not shown in the Fig. 3 because it is similar to the electron density excepted at the both sheath, which ion density is higher than the electron density responding to the voltage modulation. The sheath thickness is approximately set to 0.3 cm, and the electric potential respect the real value at the both electrodes, *e.g.* it is equal to 40 V for the phase $\pi/2$, and they are approximately equal zero for the phases 0 and π. The profile of the electric potential almost has a horizontal level in each phase, viewing the quasi-neutral characteristic of the plasma, and it is sharply inclined in the sheaths. Consequently, as shown in the electric field profile, the main electric motivating strength is positioned in the sheath.

The electron temperature profile is gain adjusted with the electrode potential variations. T_e distribution is flat in the bulk plasma and has greatest size inside the temporary cathode sheath. This is due to the ionisation rate, which latter's depends on both the electron energy and the electron density, which leads to create a peak at the temporary bulk/cathode sheath boundary, where the electron energy value is enough to make an important electron-impact ionization reaction.

To illustrate the behaviour of current discharge, we have plotted the electron, displacement, ion and total currents in Fig. 4. Despite the absent secondary

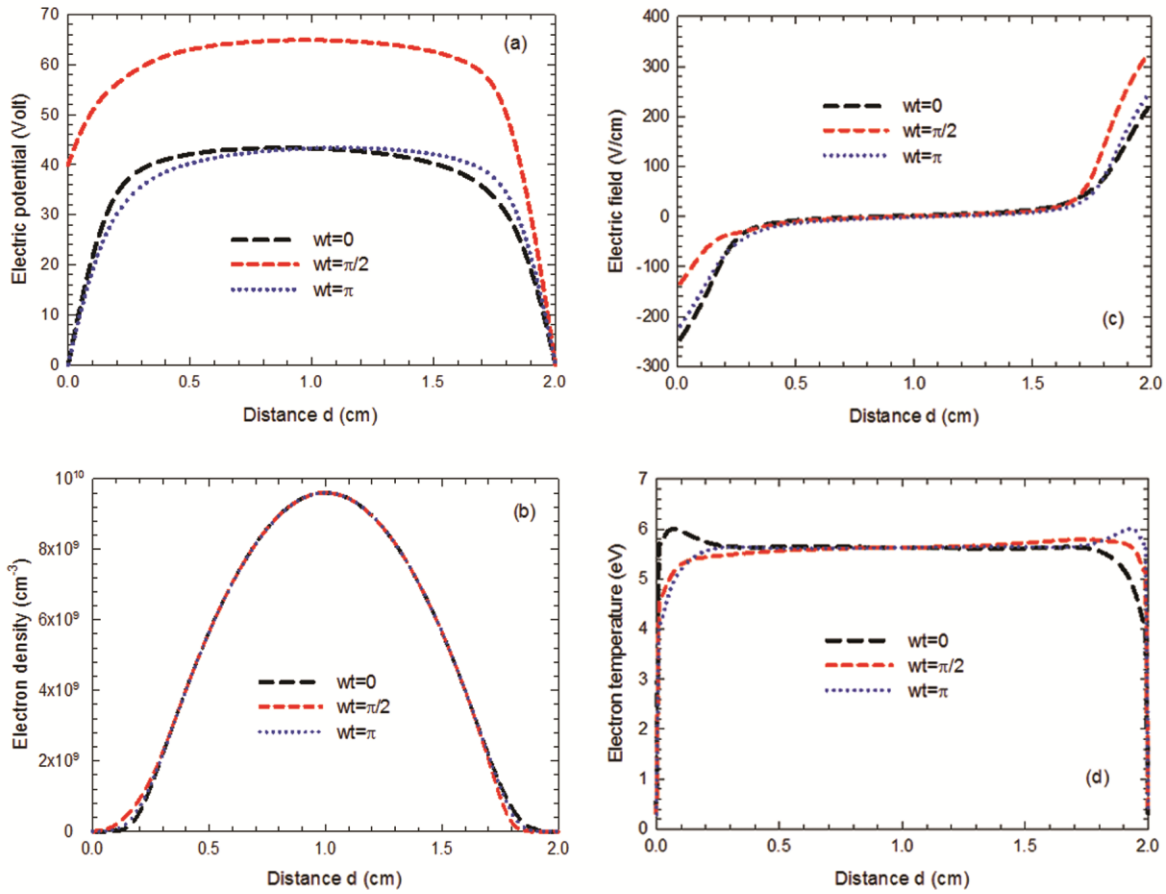

Fig. 3 — Different phases in the limit cycle (2000th cycle) of RF argon plasma representing the spatial distributions of (a) electric potential, (b) electron density, (c) electric field and (d) electron temperature.

Table 2 — Main procedures utilised in our model and that given by Lin and Adomaitis to illustrate the ccrf discharge

Our results	Results given by Lin and Adomaitis [17]
Constant spatial step	Nonuniform spatial step
Scharfetter-Gummel scheme	Pseudo spectral method
Number point in space is 200	Number point in space is 100
Full model	Model reduction
Powered electrode at the left side	Powered electrode at the right side

electron effect, quantitatively concur with the total current described in[27], and it is good agreement with Lin & Adomaitis[17] work's. Because the production of secondary electrons contributes to maintaining the discharge, to sustain the discharge, it is necessary the total current should be lower. The spatial distribution of currents again reveals the discharge physics and qualities. The profiles of ion currents amended inside the both sheaths, and are roughly linear in the bulk plasma because that the ambipolar diffusion effect is present. The spatial distributions of electron currents are important in the bulk plasma region while the displacement currents are significant in the both sheaths. As results, there is equilibrium between electrons and displacement currents. The contribution of the ion in the total currents is less, and the summation of the electron, displacement and ion currents has a constant value in all inter-electrode spacing due to the law of current preservation. In order to critic the physical phenomena's, the bulk plasma region plays a role of resistor while the both sheaths play a role of capacitors. Therefore, the current properties reveal the capacitive component of the RF argon discharge. As a result, we can simulate our reactor discharge by means of R (resistor) and C (capacitor) electrical circuit (see Refs.[28]).

(b) With dielectrics

To examine the effect of dielectrics, we have been employed the same conditions and the parameters as indicated in previous step (a: without dielectric). The procedure of simulation is again identical as

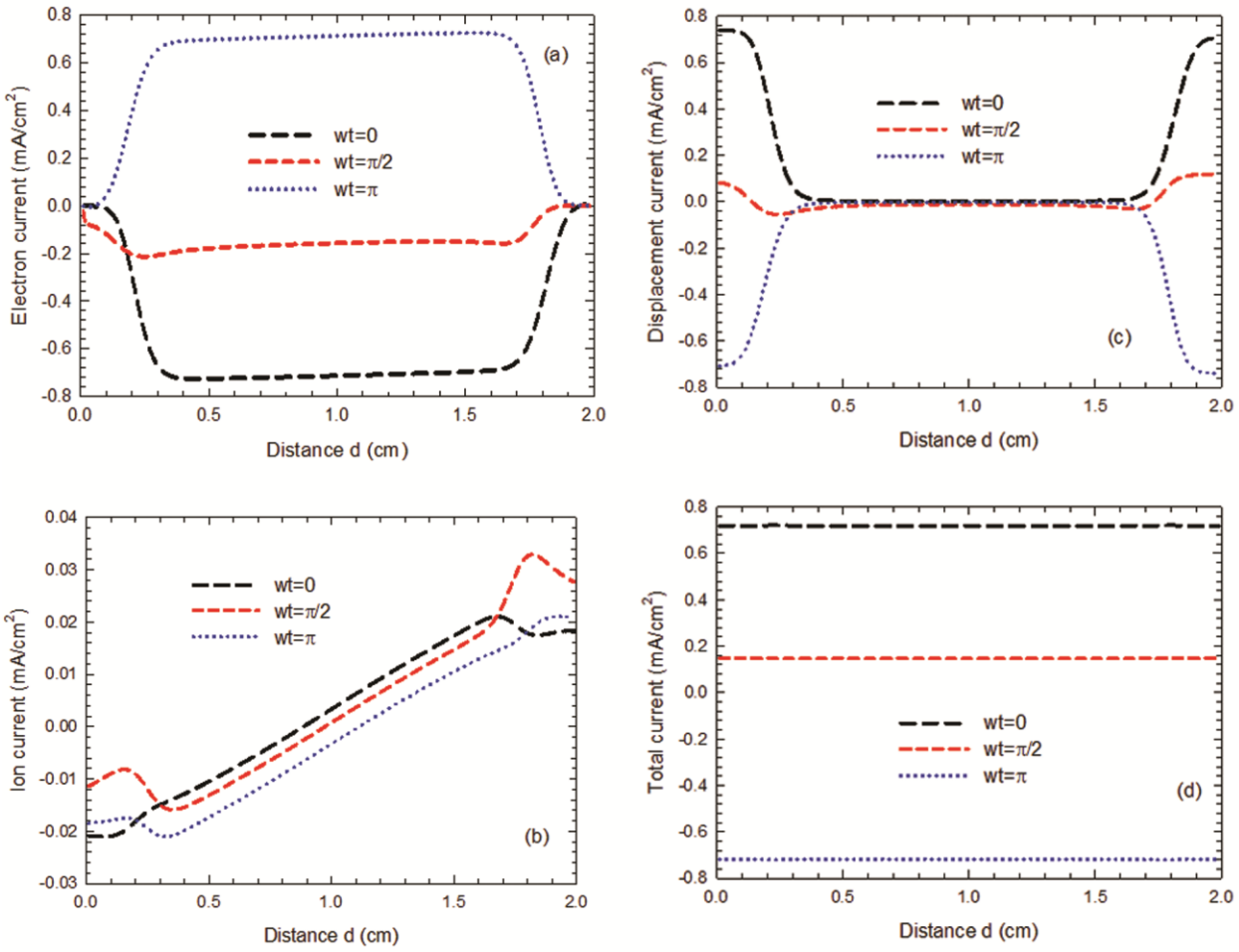

Fig. 4 — Different phases in the limit cycle (2000th cycle) of RF argon plasma representing the spatial distributions of (a) electron current, (b) ion current, (c) displacement current and (d) total current.

Table 3 — Dielectric parameters and their references

Dielectric parameters	Value	Reference
Thickness	$\Delta = 1\text{mm}$	
Relative permittivity	$\varepsilon_r = 4.6$	[16]
Reflection coefficient of electrons	$r_e = 0.7$	[13]
Reflection coefficient of ions	$r_+ = 0.005$	[13]

mentioned above; in addition we have used the boundary conditions related to the dielectrics (Equations 12-15). The dielectric is in Borofloat glass material, and it is characterised by a relative permittivity $\varepsilon_r = 4.6$ and their thickness $\Delta = 1\text{mm}$. The reflection coefficient from the dielectric of electrons $r_e = 0.7$, and of ions $r_+ = 0.005$. These parameters are reported in Table 3 with their originality.

Fig. 5 represent the spatial distribution of (a) electric potential, (b) electron density, (c) electric field and (d) electron temperature with and without dielectrics in the phase wt=0 and in the 2000th discharge cycle. As one can see from this figure the effect of the dielectrics is perceptible mostly in electric potential profile due to the both potential φ_0^t and φ_d^t, these latter created by means the accumulation of the charged particles at the sides dielectrics. The presence of the dielectrics increases the electric potential from 43.24 to 46.57 V in the bulk plasma region. Oppositely, the electron density decreases with the presence of the dielectrics because the accumulation of the charged particles at both side dielectrics diminishes the charged particles in the centre of the reactor discharge. As we can see from the electric field and the electron temperature, there are almost the same distributions with and without dielectrics. An explanation may be due to the same parameters and coefficients of the gas utilisable, then

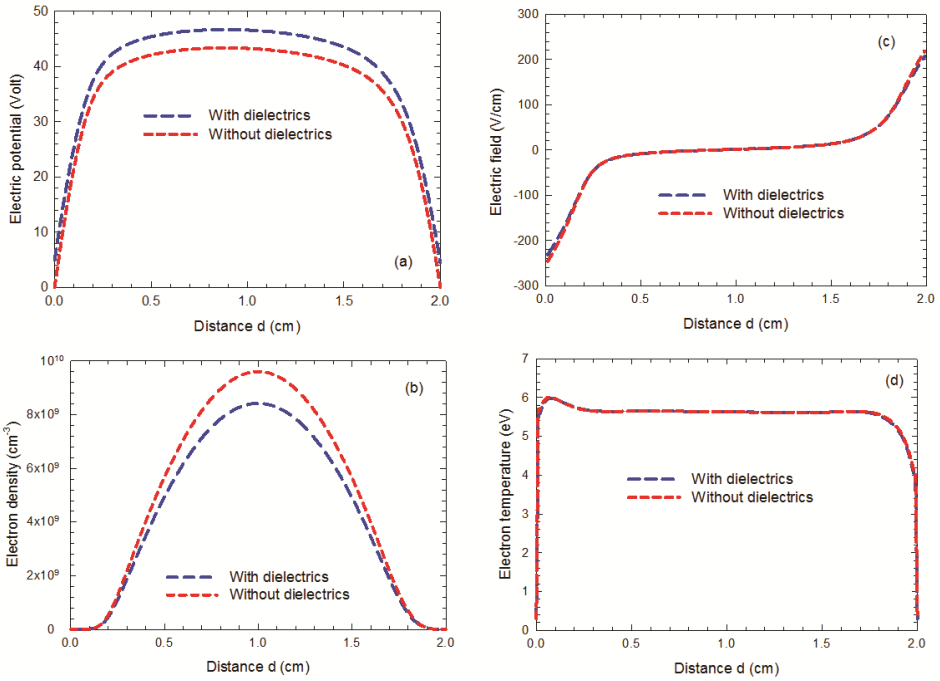

Fig. 5 — Spatial distributions of (a) electric potential, (b) electron density, (c) electric field and (d) electron temperature with and without dielectrics in the phase wt=0 and in the limit cycle (2000th cycle) of RF argon plasma.

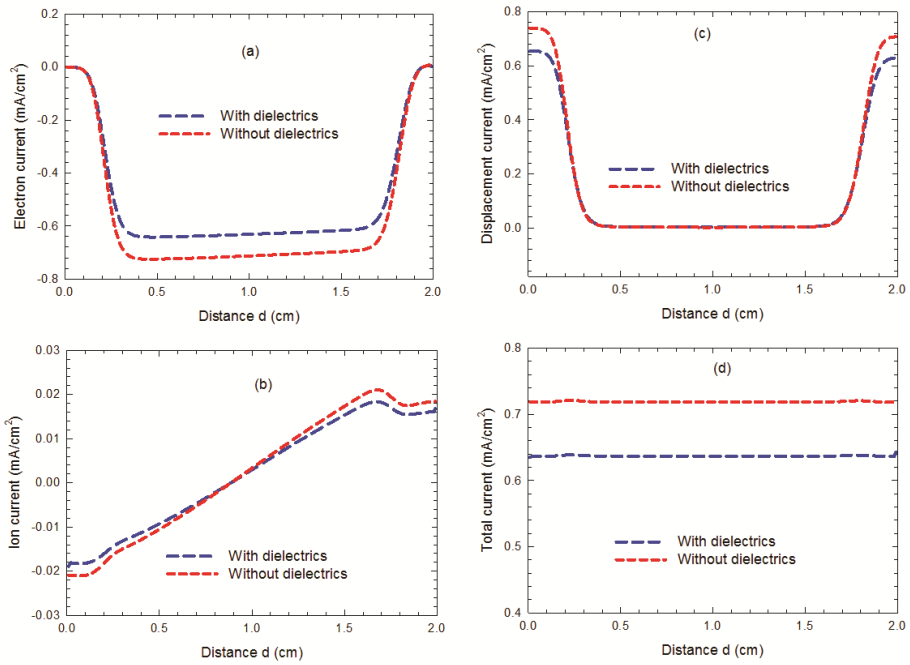

Fig. 6 — Spatial distributions of (a) electron current, (b) ion current, (c) displacement current and (d) total current with and without dielectrics in the phase wt=0 and in the limit cycle (2000th cycle) of RF argon plasma.

the same movement of particles that are present. Except at the both sides dielectrics there are minimum effects on the electric field profile.

Fig. 6 shows the spatial distributions of (a) electron current, (b) ion current, (c) displacement current and (d) total current with and without dielectrics in the phase wt=0 and in the 2000th discharge cycle. Globally, the dielectrics work to diminish the current in the reactor. It can be seen that the electron, ion and displacement currents decreases with the presence of the dielectrics. The electron current decrease in the bulk plasma region, and the both ion and displacement currents decrease at both sides' dielectrics.

Consequently, the total current decrease from 0.72 to 0.64 mA/cm^2.

Fig. 7 represents the applied and gap voltages as a function of reduced periodic of RF argon plasma in the 2000th cycle. As one can see the applied voltage U(t) is always conserved their behaviour at each period, this is evident due to the expression form of the U(t). We have defined the gap voltage $U_g(t)$: $U_g(t) = \varphi_0^t - \varphi_d^t$, as consequence the gap voltage is inferior to the applied voltage, which arrive at the maximum value about 36.3 V.

Fig. 8 shows the surface charge concentrations as a function of reduced periodic of RF argon plasma in the 2000th cycle. The morphology of the surface charge concentrations $\sigma_s(0,t)$ and $\sigma_s(d,t)$ strictly follows the gap voltage structure, and has a polarity reversal. Consequently, while the dielectric at x=0 charges at the maximum, on the other hand the dielectric at x=d charges at the minimum.

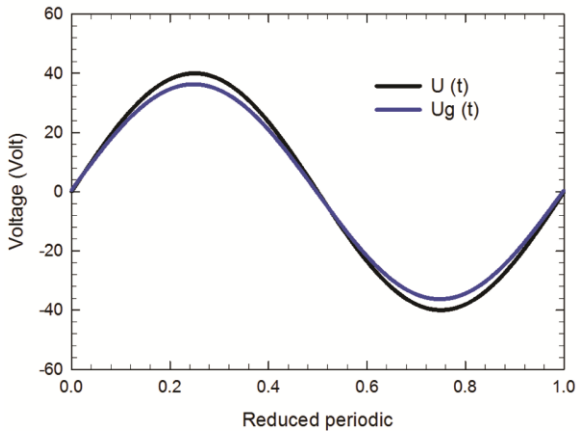

Fig. 7 — Applied and gap voltages as a function of reduced period of RF argon plasma in the 2000th cycle.

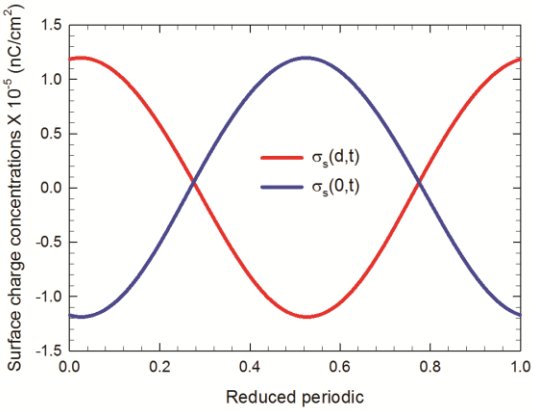

Fig. 8 — Surface charge concentrations as a function of reduced period of RF argon plasma in the 2000th cycle.

4 Conclusion

Three moments of Boltzmann's equation with Poisson's equation are taken to describe capacitively coupled argon glow discharge driven by radio frequency power at low pressure with and without dielectrics. Mainly to describe the model with dielectric, we have used the particle flux expression that can explain the kinetic of electrons and ions in the both electrodes, and the Gauss law to explain the accumulation of the charged particle on the dielectrics. The effect of boundary conditions in the presence of dielectric is well defined from the spatial distribution of the surface charge concentrations and the gap voltage temporally. As consequence the electric potential, particle densities, mean electron energy and current densities as well as the electric field are totally different compared to those obtained without dielectrics.

References

1 Becker M M, Loffhagen D & Schmidt W, *Comput Phys Commun*, 180 (2009) 1230.
2 Becker M M & Loffhagen D, *AIP Advances*, 3 (2013) 012108.
3 Alili T, Bouchikhi A & Rizouga M, *Can J Phys*, 94 (2016) 731.
4 Meyyappan M & Kreskovsky J P L, *J Appl Phys*, 68 (1990) 1506.
5 Yihung L, From detailed simulation to model reduction: development of numerical tools for a plasma processing application, Institute for Systems Research, University of Maryland, (1999).www.isr.umd.edu.
6 Yihung L & Adomaitis R A, *A global basis function approach to dc glow discharge simulation*, Technical research report, University of Maryland, USA, (1997).
7 Yihung L & Adomaitis R A, *Phys Lett A*, 243 (1998) 142.
8 Hechelef B & Bouchikhi A, *Plasma Sci Technol*, 20 (2018) 115401.
9 Bouchikhi A, *Plasma Sci Technol*, 19 (2017) 095403.
10 Bouchikhi A, *Can J Phys*, 96 (2018) 62.
11 Bouchikhi A, *IEEE Trans Plasma Sci*, 9 (2019) 4260.
12 Becker M M, Kählert H, Sun A, Bonitz M & Loffhagen D, *Plasma Sources Sci Technol*, 26 (2017) 044001.
13 Becker M M, Hoder T, Brandenburg R & Loffhagen D, *J Phys D: Appl Phys*, 46 (2013) 355203.
14 H€oft H, Kettlitz M, Becker M M, Hoder T, Loffhagen D, Brandenburg R & Weltmann K D, *J Phys D: Appl Phys*, 47 (2014) 465206.
15 Ponduri S, Becker M M, Welzel S, van de Sanden M C M, Loffhagen D & Engeln R, *J Appl Phys*, 119 (2016) 093301.
16 Loffhagen D, Becker M M, Czerny A K, Philipp J & Klages C, *Contrib Plasma Phys*, 58 (2018) 337.
17 Yihung L & Adomaitis R A, *J Comp Phys*, 171 (2001) 731.
18 Richards A D, Thompson B E & Sawin H H, *Appl Phys Lett*, 50 (1987) 492.
19 Bouchikhi A & Hamid A, *Plasma Sci Technol*, 12 (2010) 59.
20 Bouchikhi A, *Plasma Sci Technol*, 14 (2012) 965.

21 Scharfetter D L & Gummel H K, *IEEE Trans Electron Dev*, 16 (1969) 64.
22 Bouchikhi A, *Indian J Phys*, 2019.
23 Passchier J D P & Goedheer W J, *J Appl Phys*, 74 (1993) 3744.
24 Passchier J D P & Goedheer W J, *J Appl Phys*, 73 (1993) 1073.
25 Graves D B & Jensen K F, *IEEE Trans Plasma Sci*, 14 (1986) 78.
26 Meyyappan M, Ed. Computational Modeling in Semiconductor Processing (Artech House, Boston, 1995).
27 Gogolides E & Sawin H H, *J Appl Phys*, 72 (1992) 3988.
28 Belasri A & Harrache Z, *Phys Plasmas*, 17 (2010) 123501.